Characterization of Brain Abnormalities in Lactational Neurodevelopmental Poly I:C Rat Model of Schizophrenia and Depression Using Machine-Learning and Quantitative MRI

Rona Haker, MS,[1] Coral Helft, MS,[1] Emilya Natali Shamir, MS,[2] Moni Shahar, PhD,[3] Hadas Solomon, BS,[1] Noam Omer, MS,[4] Tamar Blumenfeld-Katzir, PhD,[4] Sharon Zlotzover, MS,[4] Yael Piontkewitz, PhD,[2] Ina Weiner, PhD,[1,2] and Noam Ben-Eliezer, PhD[1,4,5]* (ID)

Background: A recent neurodevelopmental rat model, utilizing lactational exposure to polyriboinosinic-polyribocytidilic acid (Poly I:C) leads to mimics of behavioral phenotypes resembling schizophrenia-like symptoms in male offspring and depression-like symptoms in female offspring.

Purpose: To identify mechanisms of neuronal abnormalities in lactational Poly I:C offspring using quantitative MRI (qMRI) tools.

Study Type: Prospective.

Animal Model: Twenty Poly I:C rats and 20 healthy control rats, age 130 postnatal day.

Field Strength/Sequence: 7 T. Multiflip-angle FLASH protocol for T_1 mapping; multi-echo spin-echo T_2-mapping protocol; echo planar imaging protocol for diffusion tensor imaging.

Assessment: Nursing dams were injected with the viral mimic Poly I:C or saline (control group). In adulthood, quantitative maps of T_1, T_2, proton density, and five diffusion metrics were generated for the offsprings. Seven regions of interest (ROIs) were segmented, followed by extracting 10 quantitative features for each ROI.

Statistical Tests: Random forest machine learning (ML) tool was employed to identify MRI markers of disease and classify Poly I:C rats from healthy controls based on quantitative features.

Results: Poly I:C rats were identified from controls with an accuracy of $82.5 \pm 25.9\%$ for females and $85.0 \pm 24.0\%$ for males. Poly I:C females exhibited differences mainly in diffusion-derived parameters in the thalamus and the medial pre-frontal cortex (MPFC), while males displayed changes primarily in diffusion-derived parameters in the corpus callosum and MPFC.

Data Conclusion: qMRI shows potential for identifying sex-specific brain abnormalities in the Poly I:C model of neurodevelopmental disorders.

Level of Evidence: NA

Technical Efficacy: Stage 2

Depression and schizophrenia are two of the most common psychiatric disorders. According to the World Health Organization, cases reach above 280 million for depression and 24 million for schizophrenia, with numbers expected to reach much higher when including undocumented cases.[1] Despite major technological advances, state-of-the-art imaging tools are limited in identifying and characterizing these conditions and report mainly structural changes.[2,3] It is clear, however, that the pathophysiology of depression and schizophrenia involves a broader range of brain abnormalities that is yet to be fully revealed.[4,5]

One of the ways to study brain abnormalities associated with depression or schizophrenia is through animal models. The anatomical and physiological parallels between humans and animals, particularly mammals, allow to investigate the antecedent risks, genetics, and early brain development, as well as test new therapies.[6,7] Recently, a new neurodevelopmental rat model—the lactational polyriboinosinic-polyribocytidilic acid (Poly I:C) model—was developed, in which lactational maternal immune activation (MIA) leads to sex-dimorphic behavioral phenotypes in the offspring, mimicking depression-like symptoms in females and schizophrenia-like symptoms in males.[8] Findings from this model align with similar epidemiologic studies, linking prenatal exposure to infection with the onset of disorders.[9] Specifically, the model by Arad et al mimics the epidemiology and pathophysiology of depression and schizophrenia via dysregulation of the mother's immune system, which, in turn, causes neuronal alterations in the newborns.[8] Validations of the prenatal Poly I:C rat model have been previously established, reflecting consistent findings that prenatal immune activation precipitates neurobiological and behavioral anomalies associated with schizophrenia and depression. Specifically, Poly I:C-induced activation of the immune response in pregnant rats led to depression and anxiety-like behaviors in offspring, alongside reduced neurotrophic support and altered tryptophan metabolism.[10] Furthermore, the model's relevance to schizophrenia has been underscored by extensive research indicating that prenatal immune challenges lead to cognitive and behavioral disruptions in the offspring, simulating the complex pathophysiology of schizophrenia.[11] These animal models parallel the human condition, where early-life infection or immune activation is epidemiologically linked to increased risks of psychiatric conditions, thereby providing important insights into the mechanisms underlying these disorders.

One of the key properties of the postnatal lactational model is its dependency on the offspring sex—similar to a sex bias in humans. Specifically, male offspring exhibit attentional and executive function abnormalities, while females exhibit depression-like symptoms of despair and anhedonia. These behavioral phenotypes were associated with volume reductions in the hippocampus and striatum in both sexes.[8] Several other groups reported neuronal differences in the prenatal MIA models of depression and schizophrenia; Ronovsky et al showed atrophy of the hippocampal dentate gyrus caused by decreased neuronal proliferation and survival rates[12]; and Wolf et al reported on neurochemical and cytoarchitectural abnormalities in the medial prefrontal cortex (MPFC) and the hippocampal dentate gyrus of Poly I:C offspring.[13] Other studies showed associations between white matter abnormalities and disease severity in animals and humans.[3,14]

Recently, a link has been demonstrated between diffusion and morphological properties of the brain vs. disease severity and symptoms, poor response to antipsychotic treatment, and worse prognosis.[15] Still, imaging-based investigation of offspring exposed to MIA is scarce, and existing studies report mainly morphological differences which are nonspecific and are present in many types of neuropsychiatric disorders.[16]

Quantitative MRI (qMRI) is an effective approach to MR imaging, whereby instead of collecting conventional contrast-weighted images, one measures the physical values underlying these contrast mechanisms to produce quantitative (numeric) maps.[17] Studies using qMRI have shown that parameters such as molecular diffusion (mean diffusivity [MD] and fractional anisotropy [FA]) and spin relaxation maps (T_1 and T_2) can be used to probe the microstructure and biochemistry of tissues with higher sensitivity than conventional contrast-weighted MRI.[18] This improves the identification of pathology in tissues that look normal and provide higher sensitivity to early microstructural changes, before noticeable abnormalities become apparent on conventional MR images.[19] No less critical, qMRI provides reproducible ground-truth values across scanners and scan settings, thereby improving their standardization and facilitating multicenter and longitudinal studies.[20]

This study aimed to assess the utility of multiregion and multiparametric qMRI markers for the characterization of neuronal abnormalities in adult female and male offspring of nursing dams injected with Poly I:C.

Materials and Methods

Animal Models

All experimental protocols conformed to the guidelines of the local Institutional Animal Care and Use Committee and NIH guidelines. Twenty male and twenty female adult Wistar rats (Harlan, Jerusalem, Israel) were kept under reversed cycle lighting (lights on 1900–0700 hours) with ad lib food and water.

At about 3 months of age, female rats were extensively handled for 5 days to habituate the animals to human handling, and then mated. Pregnant dams were housed individually, and the day of birth was defined as day 1. On postnatal day (PND) 4, whole litters were removed from the dams and placed in cages with clean bedding warmed with hot water bottles, while Poly I:C dissolved in saline (4 mg/kg/1 mL), or saline was injected intraperitoneally to the dams.

Time away from the mother was less than 3 minutes per litter. On PND 21 pups were weaned and housed 2–4 to a cage by sex and litter and maintained undisturbed until qMRI was performed in adulthood (PND 130). The tested offspring were derived from 16 Poly I:C and 15 saline litters. To control for litter effects, no more than one to two rats from the same litter were included in any of the experimental groups. The final study groups included two sex two models, based on sex (males model of schizophrenia and females model of depression), each divided into $N = 10$ Poly I:C offspring, and $N = 10$ controls, resulting in an over number of 40 animals.

MRI Scans

Scans were performed in vivo on a 7 T Bruker BioSpec scanner (Bruker Biospin, Germany), using a single-channel transmitter volume coil and a four-channel receiver head coil. Rats were anesthetized using a mixture of isoflurane (2.5%–3%) and oxygen (97.0%–97.5%). Breathing rate was monitored using a small-animal system, and body temperature was maintained at 37°C using a water circulation system.

The scan protocol and parameters are delineated in Table 1. Images were oriented coronally for all scan protocols, which included whole-brain gradient-spoiled fast low-angle shot (FLASH) using variable flip angles for quantitative estimation of longitudinal (T_1) relaxation times; a multiecho spin-echo (MESE) protocol for quantitative mapping of transverse (T_2) relaxation times; and echo-planar imaging (EPI) scan for mapping MD, FA, and the diffusion tensor. Overall scan time was 29 minutes 25 seconds per rat.

Generation of Quantitative Maps

LONGITUDINAL (T_1) RELAXATION MAPS. These maps were processed from the variable flip angle FLASH data. The acquisition included five flip angles: 3°, 6°, 10°, 15°, and 30°. T_1 values were calculated using the following signal model:

$$S = A \sin(\alpha) \frac{1 - \exp\left(-\frac{TR}{T1}\right)}{1 - \cos(\alpha) \exp\left(-\frac{TR}{T1}\right)} \quad (1)$$

where S is the acquired signal, α is the flip angle, and A denotes the local proton density (PD), weighted by the receiver coil profile (B_1^-). Before fitting, a sixth theoretical signal point was added for $\alpha = 0°$ and $S = 0$. Fitting was performed using the curve fitting tool implemented in MATLAB software (The Mathworks Inc., Natick, MA, USA).

TRANSVERSE (T_2) RELAXATION AND PD MAPS. These maps were produced from multiecho spin-echo (MESE) data using the echo modulation curve (EMC) algorithm.[21] This procedure calculates theoretical signal curves using Bloch simulations of the prospective MESE protocol. This process is repeated for a range of T_2 relaxation values and transmit-field (B_1^+) inhomogeneity levels, producing a dictionary of signal decay curves, each associated with a unique [B_1^+, T_2] value pair. The experimental signal decay curve at each voxel is then matched to the dictionary of simulated curves via minimization of the l_2-norm difference between the experimental curve and the dictionary of theoretical curves, yielding a singular T_2 value per voxel. EMC fitting was programmed in-house using

MATLAB and C++ following the algorithm described in references.[18,21]

Additional preprocessing was applied to address undesired diffusion weightings induced by the strong imaging gradients used on preclinical scanners, which may lead to significant underestimation of T_2 values. This was addressed using the algorithm presented in Bnaiahu et al, which calculates the diffusion-related attenuation for a given scan setting.[22] The EMC dictionary was accordingly adjusted to incorporate this effect, resulting in decay curves governed solely by T_2 relaxation.

DIFFUSION MAPS. MD and FA were calculated from DTI-EPI data using the ExploreDTI software package.[23] The processing pipeline included correction for subject motion and eddy currents distortions, followed by nonlinear regression to produce FA and MD maps in addition to the diffusion tensor eigenvalues λ_1, λ_2, and λ_3.

Segmentation of Brain ROIs

All quantitative maps were manually segmented by CH and TB-K (4 and 15 years of experience, respectively) using MATLAB software and a comprehensive rat brain atlas.[24] Seven two-dimensional (2D) brain regions of interest (ROIs) were marked in selected slices (see Fig. 1): cortex, corpus callosum (CC), hippocampus (Hippo.), thalamus, amygdala, MPFC, and striatum. Segmentations consisted of 2D ROIs, marked on slices, which contained the most considerable portion of each ROI. Contralateral right and left regions were combined and considered as a single region. ROIs were marked on slices at +0.7 and −3.3 from the Bregma (anterior and middle slices, respectively).

Statistical Analysis

Statistical analysis was performed using MATLAB software (version 2021b, Mathworks Inc., Natick, MA, USA), separately for females and males, relying on the sex-specificity of the behavioral deficits in the Poly I:C model.

Ten statistical parameters were extracted for each of the seven ROIs and eight qMRI maps consisting of the mean, standard deviation (SD), kurtosis, and 5, 10, 25, 50 (median), 75, 90, and 95 percentile values. To reduce partial volume effects, a single-voxel erosion was applied to each 2D ROI before feature extraction, followed by applying Chauvenet's criterion with a $3 \times$ SD margin to remove outlier values caused by fitting errors.

To identify imaging markers of the lactational Poly I:C rat model, a machine learning (ML) classifier was employed based on random forest classifier, implemented using Python's scikit-learn package. This model implements multiple decision trees and combines their predictions to improve accuracy and reduce overfitting, making it ideal for classifying subjects into two distinct groups. Each tree is trained on a random subset of the data and features (out of the training data), and the final output is determined by averaging the predictions for regression tasks or using majority voting for classification tasks. In the current study, this method was used to predict the probability that a rat belongs to either the Poly I:C or control groups by analyzing the full spectrum of collected features. The input to the classifier included 560 qMRI features calculated for seven ROIs, eight parametric maps, and 10 statistical parameters, plus seven features containing the number of voxels for each ROI.

Table 1. Scan Protocols and Experimental Parameters

Protocol	Time (minutes: seconds)	TR (msec)	TE (msec)	Field of View (mm³)	Resolution (mm²)	Slice Thickness (mm)	Averages	Flip Angle (degrees)	BandWidth (kHz)	Comments
FLASH	2:46 1:23	25	2.8	24.0 × 19.2 × 20.8	0.15 × 0.15	0.8	2 1	3 6, 10, 15, 30	50	
MESE	10:14	3200	5.9 ETL = 20	24.0 × 19.2	0.15 × 0.15	0.8	2	90	50	Partial Fourier = ×1.34
EPI-DTI	9:20	4000	19.2	24.0 × 19.2	0.267 × 0.267	0.8	2	90	50	32 directions, b-value = 0, 1000

The MRI sequences used in this study and their parameters are described in this table. The total scan time was 29 minutes 25 seconds per rat.

Classification was followed by performing pairwise Pearson correlation between each pair of features in order to assess whether features overlapped or contained complementary information. Diffusion weighted data of two of the male rats (one from the Poly I:C and one from the control group) was corrupted, presumably due to mispositioning of the transceiver coil. As the random forest ML model requires full data, the corresponding features for the diffusion maps were replaced by the group average for each of the 10 statistical parameters similar to Steyerberg and van Veen.[25]

Data were separated into a train set (15 rats), validation set (3 rats), and test set (2 rats). During training, the model used the train and validation data to assign weights to each of the statistical features so as to iteratively maximize the prediction accuracy for the validation data. Once this was done, the ensuing weights were used to calculate the model's accuracy on the test data. Due to the small sample size full cross-validation was performed by training the model on all possible separations of the data into train + validation, and test. Specifically, data for one out of 10 Poly I:C animals and one out of 10 control animals were set aside as a test set, resulting in 100 possible permutations. This methodology ensured that the model's inferences were based on the entirety of the available dataset, thereby maximizing its predictive ability and minimizing its dependency on specific choice of separating into train and test. The final accuracy was ultimately calculated as the average accuracy across all 100 permutations.

Each classification produced a number between 0 and 1, while the confidence level was determined based on how far or close was the prediction from a threshold of 0.5 between Poly I:C and control groups. To assess the confidence level of true positive (TP) vs. false positive (FP) predictions and of true negative (TN) vs. false negative (FN) predictions a two-tailed t test was performed between each series of predictions, and within each sex group.

Model optimization included three hyperparameters: the number of decision trees which was set on 500 after testing the range of 50, 200, 500, 1000; the number of animals used for test, which was set at a minimal number of "1" due to the small cohort size; and the classification threshold, which chosen to get a default value of 0.5 seeing as optimizing this parameter for such small cohort might improve the fitting simply due to overfitting.

Estimation of Features' Importance

The relative contribution of each ROI and quantitative map to the identification of pathology in Poly I:C animals was estimated based on output from the random forest classifier. This was done by averaging the importance of each feature as reported by the ML model (range = 0–100), across the hundred permutations of separating the data into train and test.

Results

Quantitative MRI Maps

Representative T_1, T_2, and diffusion-weighted images for a female Poly I:C rat are shown in Fig. 2 for two brain segments located at −3 and +0.7 from the Bregma. Corresponding T_1, T_2, FA, and MD maps, calculated from these images, are shown in Fig. 3, after skull stripping and for the same two locations. Notably, the signal bias caused by the
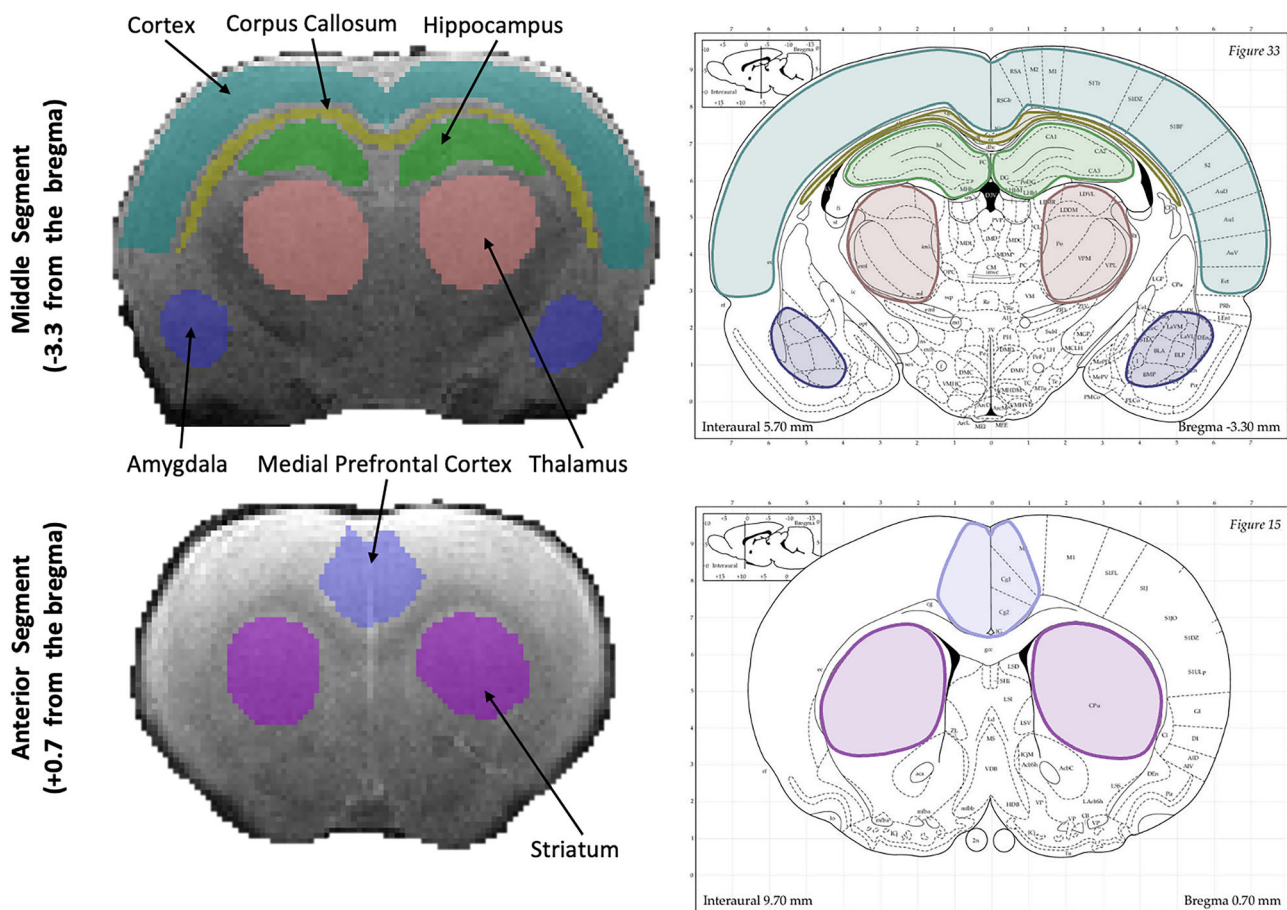
Figure 1: Brain regions of interest (ROIs) segmentation overlaid on T_1-weighted images. Seven ROIs were manually segmented on 2D T_1-weighted images including: cortex, corpus callosum (CC), hippocampus (Hipp.), thalamus, amygdala, medial prefrontal cortex (MPFC), and striatum.

receiver coil profile seen in the contrast-weighted images in Fig. 2 affected all images in the series similarly. This means that the fitting algorithms should be able to "see through" this bias field, and thus are not expected to be influenced by this bias field, except a decrease in the images and maps' singal to noise ratio (SNR) in regions that are farther from the coils.

Discrimination Between Poly I:C and Control Rats Based on Random Forest Classifier

The classifier output consisted of a numeric score in the range 0–1 (control or Poly I:C), with a threshold of 0.5 used to classify animals between the two groups. The overall model accuracy on the test data was $82.5 \pm 25.9\%$ for females with 88% sensitivity and 77% specificity, and an accuracy of $85.0 \pm 24.0\%$ for males with 90% sensitivity and 80% specificity. A slightly lower accuracy was exhibited on the training data producing $79.2 \pm 6.7\%$ for females and $80.2 \pm 5.2\%$ for males, indicating that the model did not overfit the training data. Specific prediction scores are shown in Fig. 4 for both males and females for all hundred permutations of

separating the data into train and test. A numerical summary of the classification performance appears in Table 2, delineating the absolute number of TP, FP, TN, and FN predictions for females and males. Random forest prediction scores were statistically higher for TP than for FP for both females and males (top parts of Fig. 4, $P < 0.001$ for both sexes), indicating that the model had higher confidence in true than for in false predictions. Similarly, the prediction scores of TN were statistically lower than FN predictions for both females and males (bottom parts of Fig. 4, $P < 0.001$ for both sexes).

Features' Importance

The importance of each ROI and quantitative map to the classification process is presented in Table 3. As can be observed, some ROIs and maps were consistently more indicative to the state of the rats (control or Poly I:C), while other [ROI, map] combinations were much less informative to the model. For both males and females classification relied mainly on diffusion-derived maps with high involvement of FA in the thalamus and λ_2 and λ_3 in the MPFC. Males exhibited the highest reliance on FA in the MPFC and in the
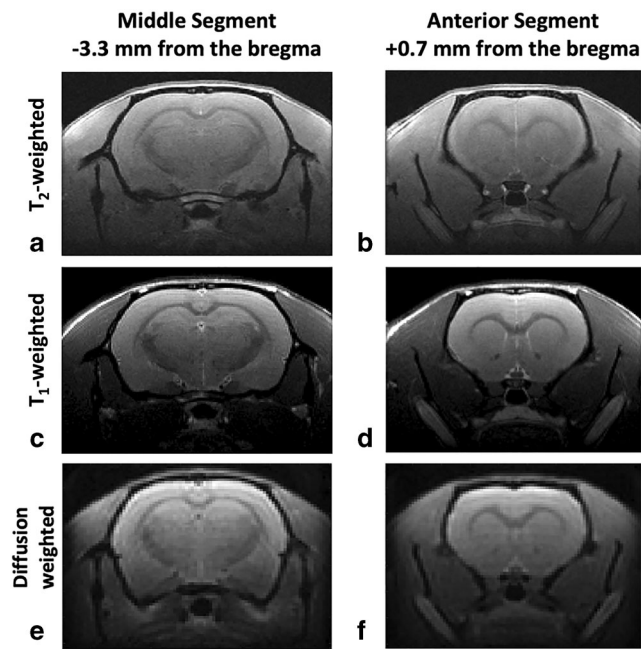
5

Figure 2: Representative contrast-weighted images of a Poly I:C rat brains, used for calculation of quantitative MRI (qMRI) maps. Images are shown for two slices located at positions −3.3 and +0.7 mm from the bregma. (a, b) Multiflip-angle T_1-weighted FLASH images (flip angle = 10°), used for the calculation of T_1 maps. (c, d) MESE T_2-weighted images (TE = 5.9 msec) used for calculation of T_2 and PD maps. (e, f) Diffusion-weighted images collected using an EPI-DTI protocol (b-value = 0), used for calculation of FA, MD, and λ_1, λ_2, and λ_3 maps.

CC. Water density (PD) and relaxation-derived metrics exhibited lower average importance, with moderate involvement of T_2 in classification of the female model of depression.

Pairwise Correlation Between qMRI Features

Full pairwise correlations between each pair of features are shown in Fig. 5. The analysis highlights three main findings: first, that the set of metrics within each quantitative map is internally correlated, with the highest internal correlation appearing in the T_1 map. Second, is that there is high correlation between diffusion-derived values with no visually apparent difference in the correlation between the five maps assayed. Third, and perhaps the most striking feature, is the relatively lower correlation between the four different contrast mechanisms, that is, diffusion, PD, T_1 and T_2, indicating that these provide complementary information.

Discussion

This study utilized a new set of qMRI markers to characterize brain pathology in adult female and male rats that were exposed to MIA in lactation. A multiparametric ML model is capable of identifying pathology in Poly I:C rats vs. healthy controls with high accuracy. Importantly, this diagnostic model considers both brain region, and animal sex, similar to models of depression and schizophrenia in humans.[26]

Various methodologies have been proposed for the characterization of psychiatric disorders. The added value of using qMRI to investigate tissue pathology is threefold. First, it offers higher sensitivity to subtle tissue differences that cannot be visually observed on conventional images, and are beyond straightforward morphological changes.[27] Second, the numeric nature of qMRI markers allows the use of ML models, which would be less effective when relying on *qualitative* contrast-weighted images. Lastly, qMRI values have higher reproducibility across scanners and scan settings,
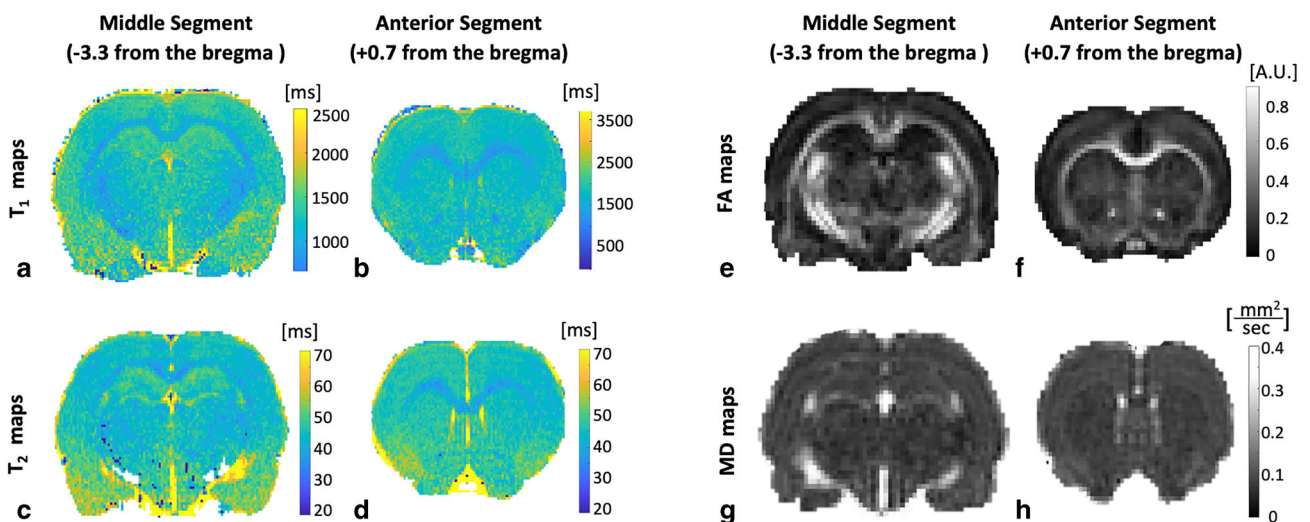
Figure 3: Representative quantitative T_1, T_2, FA, and MD maps. Maps are shown for two slices located at positions −3.3 and +0.7 mm from the bregma. (a, b) Quantitative T_1 maps generated using a multiflip-angle FLASH protocol (see Eq. 1). (c, d) Quantitative T_2 maps derived from a MESE protocol and processed using the EMC algorithm.[18,21] (e, f) Fractional anisotropy (FA) maps obtained from an EPI-DTI protocol. (g, h) Mean diffusivity (MD) maps obtained from an EPI-DTI protocol. Both FA and MD values were computed using ExploreDTI software.[23]

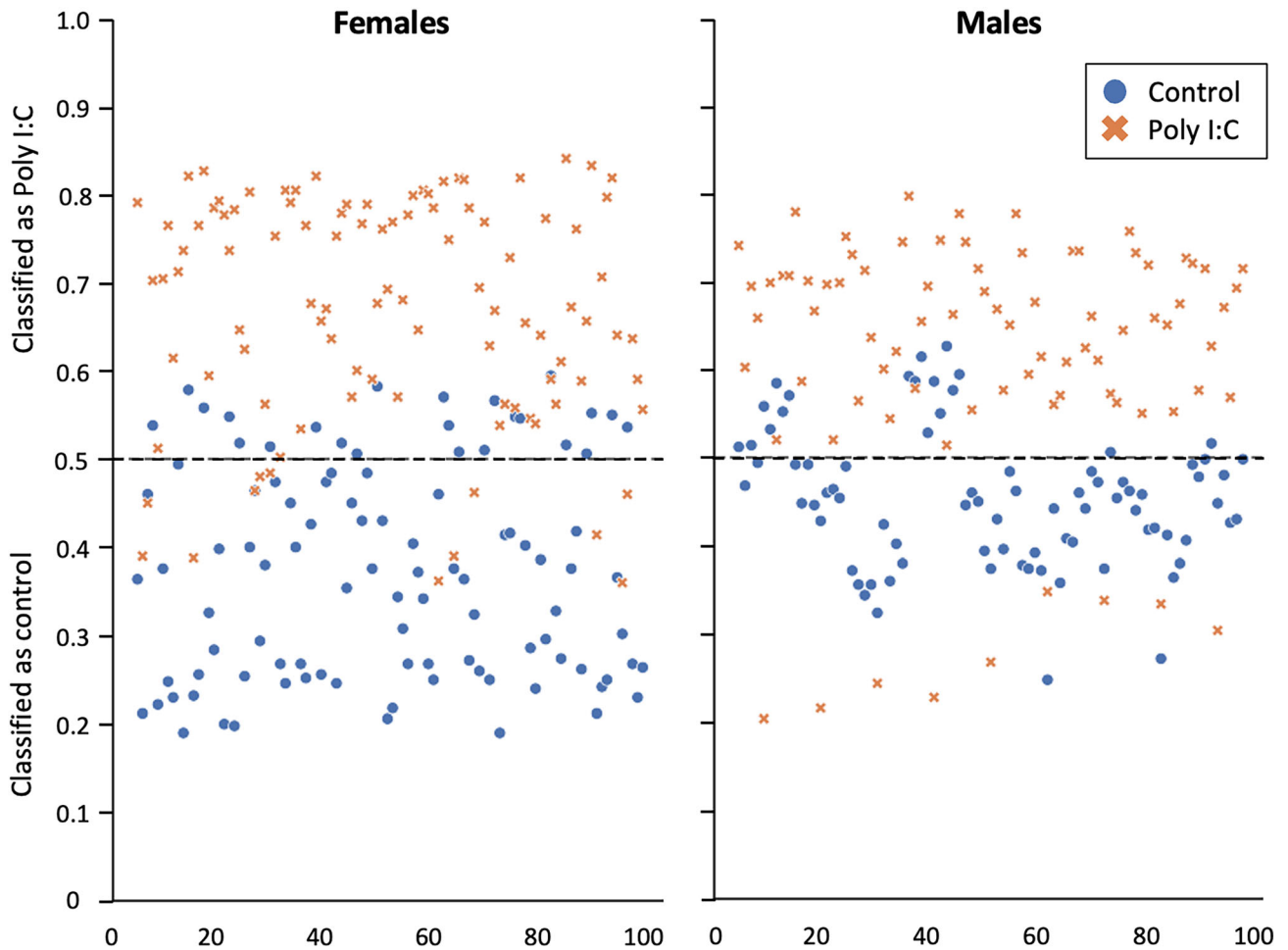Figure 4: Classification of the machine learning model, across all 100 cross-validation permutations. Accuracy of 82.5 ± 25.9% for females and 85.0 ± 24.0% for males was achieved using a random forest machine learning classifier. This figure also provides a visual depiction of the confidence levels associated with each prediction, contingent to their respective classifications and distance from the 0.5 threshold value.

Table 2. Confusion Matrix for Random Forest Output

		Females		Males	
		Predicted		**Predicted**	
		Poly I:C	**Control**	**Poly I:C**	**Control**
Actual	Poly I:C	88	12	90	10
	Control	23	77	20	80

Confusion matrix summarizing the machine learning classification of Poly I:C vs. control rats. Values are shown for 200 predictions for females and 200 for males (100 permutations of the data to train and test, two animals per run). Classification accuracy was 82.5% (165 out of 200) for females, and 85.0% (170 out of 200) for males.

thereby promoting standardization of the ensuing imaging markers.[28]

The presented approach of probing multiple brain regions and qMRI contrasts expands on previous characterizations of the Poly I:C model, which primarily reported differences in striatal and hippocampal volumes.[8] To cope with the large number of quantitative features a random forest model was employed, which can process hundreds of input parameters. By this, this classifier can overcome redundancy of information across markers from different regions/maps, while mitigating the penalty incurred by using a large number of features, leading to higher predictive power.[29] Another

Table 3. Feature Importance by Brain Region of Interest and qMRI Map

		T_1	PD	T_2	FA	λ_1	λ_2	λ_3	MD	N-vox.	
Females	Cortex	2.6	12.3	14.5	5.8	4.5	5.6	6.1	4.1	1.5	
	CC	5.8	11.6	4.3	10.6	7.6	5.6	8.3	8.4	0.4	100
	Hipp.	4.4	4.8	33.6	2.9	3.6	2.3	7.7	5.6	0.6	90
	Thalamus	4.8	3.6	5.4	96.6	52.2	41.3	38.4	13.8	2.0	80
	Amygdala	5.1	5.5	29.1	2.3	6.3	7.7	4.7	3.0	2.0	70
	MPFC	2.9	7.5	24.0	37.4	45.2	78.6	115.2	47.0	0.5	60
	Striatum	3.7	4.1	34.9	6.3	12.2	42.6	16.7	9.2	3.0	50
Males	Cortex	4.4	8.3	5.4	19.0	10.8	9.0	23.2	14.2	3.7	40
	CC	4.5	4.2	9.1	114.0	34.1	6.1	4.2	16.6	0.8	30
	Hipp.	7.0	3.4	6.2	8.6	11.0	38.7	6.9	15.4	0.7	20
	Thalamus	7.2	2.8	6.7	22.9	8.3	11.5	8.1	20.1	1.8	10
	Amygdala	5.5	4.2	6.7	10.5	3.1	4.1	4.4	4.5	0.6	0
	MPFC	3.5	8.0	5.1	118.6	78.3	24.9	15.7	48.6	0.5	
	Striatum	5.5	11.2	6.2	6.5	15.7	51.6	48.0	29.4	0.6	

Relative importance of qMRI features for classification between Poly I:C and control rats. Values are shown per brain region and qMRI map. Scale is 0–1000 (with a maximal value of ~120) and corresponds to the average importance of each [ROI, qMRI map] in the random forest model. Upper part of the table pertains to females, while the lower refers to males.

CC, corpus callosum; Hipp., hippocampus; MPFC, medial prefrontal cortex.

important property of this ML model is the use of multiple decision trees which helped reduce data overfitting that might have improved the classification of training data at the cost of lower accuracy on the unseen test data. To fully utilize the amount of data collected in the study, a comprehensive cross-validation procedure was implemented whereby all possible permutations of dividing the data into train and test were applied. This promoted the robustness of the model and ensured that it will not be dependent on the specific choice of train and test sets.

Results indicate that the behavioral differences between male and female Poly I:C rats, shown previously by Arad et al, are also reflected in imaging findings, similar to the manifestation of these conditions in humans.[8] These sex differences were reflected both in quantitative values and brain regions, whose relevance to pathology was estimated as the average importance of each [map, ROI] combination across all possible separations of the data to train and test (total of $N = 100$ permutations). Results show that, overall, tissue integrity was the main driving factor as reflected by differences in diffusion-derived values, with moderate effect of T_2

relaxation times in the females, possibly indicating an underlying inflammatory process.

The classification of the Poly I:C female model of depression relied primarily on differences in the thalamus and MPFC, known to play a role in regulating cognitive and emotional processes.[30,31] Molecular diffusion was the most affected mechanism, having the largest contribution to the classification. Specific findings included strong involvement of FA in the thalamus in the classification process, reflecting an underlying decrease in FA and increase in MD, suggestive of disrupted neuronal integrity and connectivity, thereby impairing its role as a relay station for relegating information between different brain regions.[31] Poly I:C group also exhibited an increase of mean and SD (heterogeneity) of the diffusivity in the MPFC, which is responsible for the processing of emotions and social withdrawal, and in the striatum, which may cause an imbalance in the reward system and biased processing of negative information.[32,33] Lastly, T_2 relaxation times also contributed to the classification. This may result from an increases of T_2 in the cortex, hippocampus, striatum and MPFC, associated with reduced
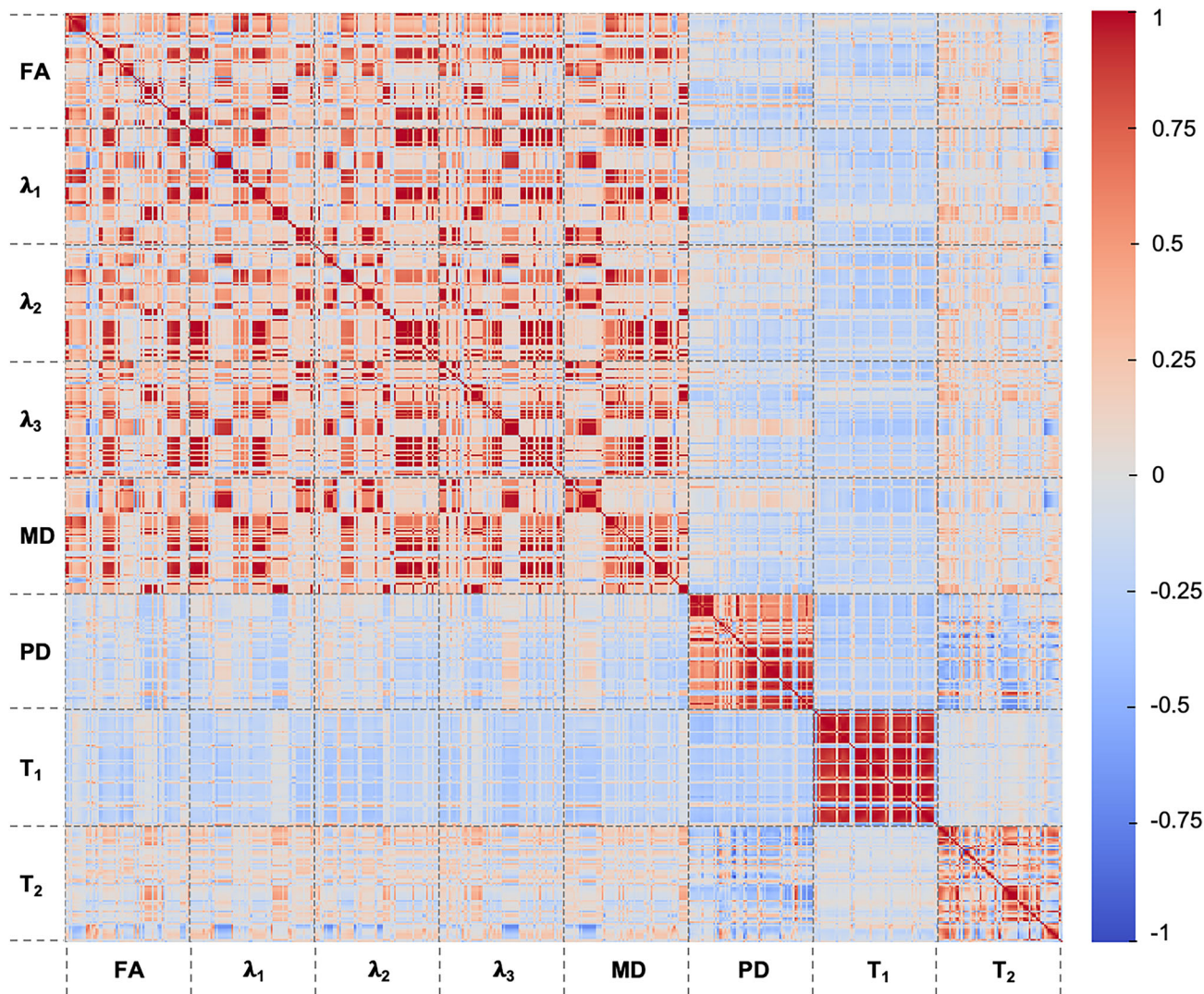
RIGHTS LINK

Figure 5: Pairwise correlation between qMRI features per region and map type. The degree of overlap between features is color coded between 0 (no correlation) and +1/−1 (perfect positive/negative correlation). Relatively high internal correlation is observed between the subset of diffusion-related values (FA, MD, and diffusion tensor eigenvalues), and within relaxation derived maps (T$_1$, T$_2$, and PD), with low correlation between different contrast mechanisms, suggesting that these data are complementary to one another.

myelination or subtle inflammation, which is typical in depressive disorders.[34]

Differences in MRI markers of male rat models of schizophrenia were observed mainly in the corpus callosum, and MPFC. These were primarily seen in diffusion-derived markers, which manifest a decrease in tissue integrity at the macro- or microstructural levels. The corpus callosum is the largest white matter structure in the brain, regulating thought, emotional, and behavioral processes.[35] The reduction in FA was seen in this region is congruent with impaired axonal integrity and decreased connectivity. This may relate to dysfunctional cortical circuitry associated with impairments in attention, memory, and executive functions, which have been widely recognized as core aspects of schizophrenia.[36–38] Such behavioral differences may also be linked to a decrease in MD seen in the cortex, again, suggesting impaired tissue

integrity associated with cell swelling, increased membranal permeability, or demyelination.[39–41]

Study Limitations

First, the small cohort size limits the ability to estimate the importance of each feature. Although all possible permutations of separating the data to train + validation and test were considered, the relatively limited number of animals means that the importance of each feature could only be assessed, thereby affecting the generalizability of the model. Larger cohorts are thus necessary to further verify these results, and particularly their neurological interpretation and translational applicability. Second, although the ROIs-based approach is advantageous for small datasets, it might mask localized, intra-ROI differences, which can only be captured using pixel-wise analyses like z-score or using histopathology.[42] An

example of this is the thalamus, which is comprised of multiple subthalamic nuclei, associated with different neurological functions. Anterior thalamic nuclei are necessary for spatial navigation and memory, whereas the mediodorsal thalamus is necessary for executive control, memory, and reward processing.[43,44] Treating the thalamus as an indivisible entity may thus obscure effects within specific subnuclei, potentially misrepresenting its significance in classification. Lastly, the use of a surface head coil in the MRI scans introduces variability of the transmit and receive fields (B_1^+ and B_1^- respectively), leading to higher SNR close to the coil and lower SNR in more inferior regions, like the striatum, thalamus and particularly the amygdala. This leads to higher SD (i.e., lower precision) in qMRI values in these regions, which may propagate into the ML model.

Conclusions

The current study demonstrates the utility of qMRI in characterizing sex-specific brain abnormalities in a neurodevelopmental rat model of schizophrenia and depression induced by maternal Poly I:C exposure. The application of multiparametric MRI and ML classifier enabled accurate differentiation of Poly I:C-affected rats from controls, with significant reliance on diffusion-derived markers for both females and males. Findings reveal sex-specific alterations in brain regions related to emotional regulation, cognition, and behavior, highlighting the potential of qMRI as a tool for early detection and investigation of psychiatric disorders in both clinical and research settings.

Conflict of Interest

Authors have nothing to disclose.

References

1. World Health Organization. *Depression and other common mental disorders*. Geneva: World Health Organization; 2017.

2. Goodkind M, Eickhoff SB, Oathes DJ, et al. Identification of a common neurobiological substrate for mental illness. JAMA Psychiatry 2015;72: 305-315.

3. Zhuo C, Li G, Lin X, et al. The rise and fall of MRI studies in major depressive disorder. Transl Psychiatry 2019;9:335.

4. Cui L, Li S, Wang S, et al. Major depressive disorder: Hypothesis, mechanism, prevention and treatment. Signal Transduct Target Ther 2024; 9:30.

5. Tandon R, Nasrallah H, Akbarian S, et al. The schizophrenia syndrome, circa 2024: What we know and how that informs its nature. Schizophr Res 2024;264:1-28.

6. Reisinger S, Khan D, Kong E, Berger A, Pollak A, Pollak DD. The Poly(I:C)-induced maternal immune activation model in preclinical neuropsychiatric drug discovery. Pharmacol Ther 2015;149:213-226.

7. Barré-Sinoussi F, Montagutelli X. Animal models are essential to biological research: Issues and perspectives. Future Sci OA 2015;1:FSO63.

8. Arad M, Piontkewitz Y, Albelda N, Shaashua L, Weiner I. Immune activation in lactating dams alters sucklings' brain cytokines and produces non-overlapping behavioral deficits in adult female and male offspring: A novel neurodevelopmental model of sex-specific psychopathology. Brain Behav Immun 2017;63:35-49.

9. Meyer U. Developmental neuroinflammation and schizophrenia. Prog Neuropsychopharmacol Biol Psychiatry 2013;42:20-34.

10. Gibney SM, McGuinness B, Prendergast C, Harkin A, Connor TJ. Poly I:C-induced activation of the immune response is accompanied by depression and anxiety-like behaviours, kynurenine pathway activation and reduced BDNF expression. Brain Behav Immun 2013;28:170-181.

11. Meyer U, Feldon J. To poly(I:C) or not to poly(I:C): Advancing preclinical schizophrenia research through the use of prenatal immune activation models. Neuropharmacology 2012;62:1308-1321.

12. Ronovsky M, Berger S, Molz B, Berger A, Pollak D. Animal models of maternal immune activation in depression research. Curr Neuropharmacol 2016;14:688-704.

13. Wolf S, Mattei D, Schweibold R. Brain in flames – animal models of psychosis: Utility and limitations. Neuropsychiatr Dis Treat 2015;11:1313.

14. Xu H, Li X-M. White matter abnormalities and animal models examining a putative role of altered white matter in schizophrenia. Schizophr Res Treat 2011;2011:1-16.

15. Kraguljac NV, McDonald WM, Widge AS, Rodriguez CI, Tohen M, Nemeroff CB. Neuroimaging biomarkers in schizophrenia. Am J Psychiatry 2021;178:509-521.

16. Brown AS, Meyer U. Maternal immune activation and neuropsychiatric illness: A translational research perspective. Am J Psychiatry 2018; 175(11):1073-1083. https://doi.org/10.1176/appi.ajp.2018.17121311.

17. Ben-Eliezer N. Advances in signal processing for relaxometry. *Advances in magnetic resonance technology and applications*, Vol 1: Elsevier, London; 2020. p 123-147.

18. Radunsky D, Stern N, Nassar J, Tsarfaty G, Blumenfeld-Katzir T, Ben-Eliezer N. Quantitative platform for accurate and reproducible assessment of transverse (T_2) relaxation time. NMR Biomed 2021;34:e4537.

19. Shepherd TM, Kirov II, Charlson E, et al. New rapid, accurate T_2 quantification detects pathology in normal-appearing brain regions of relapsing-remitting MS patients. NeuroImage Clin 2017;14:363-370.

20. Gracien R-M, Maiworm M, Brüche N, et al. How stable is quantitative MRI?—Assessment of intra- and inter-scanner-model reproducibility using identical acquisition sequences and data analysis programs. Neuroimage 2020;207:116364.

21. Ben-Eliezer N, Sodickson DK, Block KT. Rapid and accurate T_2 mapping from multi–spin-echo data using Bloch-simulation-based reconstruction. Magn Reson Med 2015;73:809-817.

22. Bnaiahu N, Omer N, Wilczynski E, Levy S, Blumenfeld-Katzir T, Ben-Eliezer N. Correcting for imaging gradients–related bias of T_2 relaxation times at high-resolution MRI. Magn Reson Med 2022;88: 1806-1817.

23. Leemans A, Jeurissen B, Sijbers J, Jones DK. ExploreDTI: A graphical toolbox for processing, analyzing, and visualizing diffusion MR data. https://www.exploredti.com/

24. Rat Brain Atlas. Available from: https://labs.gaidi.ca/rat-brain-atlas/

25. Steyerberg EW, van Veen M. Imputation is beneficial for handling missing data in predictive models. J Clin Epidemiol 2007;60:979.

26. Samsom JN, Wong AHC. Schizophrenia and depression co-morbidity: What we have learned from animal models. Front Psychiatry 2015;6:6.

27. Solomon C, Shmueli O, Shrot S, et al. Psychophysical evaluation of visual vs. computer-aided detection of brain lesions on magnetic resonance images. Magn Reson Imaging 2023;58:642-649.

28. Gulani V, Seiberlich N. Quantitative MRI: Rationale and challenges. In: Seiberlich N, Gulani V, Calamante F, et al., editors. *Advances in magnetic resonance technology and applications*, Vol 1: Elsevier, London; 2020. p xxxvii-li.

29. Pudjihartono N, Fadason T, Kempa-Liehr AW, O'Sullivan JM. A review of feature selection methods for machine learning-based disease risk prediction. Front Bioinform 2022;2:927312.

30. Xu P, Chen A, Li Y, Xing X, Lu H. Medial prefrontal cortex in neurological diseases. Physiol Genomics 2019;51:432-442.

31. Yang C, Xiao K, Ao Y, Cui Q, Jing X, Wang Y. The thalamus is the causal hub of intervention in patients with major depressive disorder: Evidence from the Granger causality analysis. NeuroImage Clin 2023; 37:103295.

32. Ng TH, Alloy LB, Smith DV. Meta-analysis of reward processing in major depressive disorder reveals distinct abnormalities within the reward circuit. Transl Psychiatry 2019;9:293.

33. Kupferberg A, Bicks L, Hasler G. Social functioning in major depressive disorder. Neurosci Biobehav Rev 2016;69:313-332.

34. Sacchet MD, Gotlib IH. Myelination of the brain in major depressive disorder: An in vivo quantitative magnetic resonance imaging study. Sci Rep 2017;7:2200.

35. Schutter DJLG, Harmon-Jones E. The corpus callosum: A commissural road to anger and aggression. Neurosci Biobehav Rev 2013;37:2481-2488.

36. Smucny J, Dienel SJ, Lewis DA, Carter CS. Mechanisms underlying dorsolateral prefrontal cortex contributions to cognitive dysfunction in schizophrenia. Neuropsychopharmacology 2022;47:292-308.

37. Gao W-J, Yang S-S, Mack NR, Chamberlin LA. Aberrant maturation and connectivity of prefrontal cortex in schizophrenia—Contribution of NMDA receptor development and hypofunction. Mol Psychiatry 2022; 27:731-743.

38. Giraldo-Chica M, Rogers BP, Damon SM, Landman BA, Woodward ND. Prefrontal-thalamic anatomical connectivity and executive cognitive function in schizophrenia. Biol Psychiatry 2018;83: 509-517.

39. Concha L. A macroscopic view of microstructure: Using diffusion-weighted images to infer damage, repair, and plasticity of white matter. Neuroscience 2014;276:14-28.

40. Aung WY, Mar S, Benzinger TL. Diffusion tensor MRI as a biomarker in axonal and myelin damage. Imaging Med 2013;5:427-440.

41. Wegrzyn D, Juckel G, Faissner A. Structural and functional deviations of the hippocampus in schizophrenia and schizophrenia animal models. Int J Mol Sci 2022;23:5482.

42. Ulug AM, Ozkan M, Kingsley PB, et al. Multi-contrast z-score comparison discriminates patients with psychiatric disorders from controls. Proc Intl Soc Mag Reson Med 2015;23:3561.

43. Saalmann YB. Intralaminar and medial thalamic influence on cortical synchrony, information transmission and cognition. Front Syst Neurosci 2014;8:8.

44. Jankowski MM, Ronnqvist KC, Tsanov M, et al. The anterior thalamus provides a subcortical circuit supporting memory and spatial navigation. Front Syst Neurosci 2013;7:7.